of certain nucleic acids. Some of these issues parallel those of the preceding chapters, where more emphasis was placed on proteins and polypeptides. The book concludes in Chapter 25 with a shift to the important subject of membrane equilibria and the structure and behavior of lipid bilayers.

Of course, much of the material in Part III is tied closely to the discussion in Parts I and II. In appropriate places, reference is made to the earlier chapters. However, many readers will find it possible to read a good portion of this Part without having read the other Parts, particularly if the appropriate section of an earlier chapter is consulted when needed.

15
Ligand interactions at equilibrium

15-1 IMPORTANCE OF LIGAND INTERACTIONS

A wide variety of physiological processes are the reflection of ligand interactions with macromolecules, especially with proteins. The most common are interactions between enzymes and their substrates and with other molecules that influence activity. In addition, there are interactions between hormones and hormone receptors, between small molecules and proteins involved in the active transport of the small molecules, between ions and both nucleic acids and proteins, and so on. Upon reflection, it is clear that virtually all biological phenomena depend on one or more ligand interactions. It is not surprising, therefore, that a large amount of biochemical and biophysical research has been directed at exploring these interactions in depth.

Our first consideration is to develop the statistical framework that enables us to treat (and to gain insight into) the principal features of an equilibrium ligand association system. These are general considerations that apply to any equilibrium system. In addition, there are many special features, such as site–site interactions and cooperativity, linkage relationships between two different ligands binding to the same macromolecule, and statistical complications associated with linear, latticelike chains.

General features of ligand interactions at equilibrium are developed in this chapter; Chapter 16 treats kinetic phenomena. In addition, Chapters 16 and 17 deal with some of the special areas that play a prominent role in biochemistry. These include enzymatic systems (Chapter 16) and regulation phenomena (Chapter 17) commonly known as allosteric interactions. The treatment of some of these issues draws on the general framework laid down in this chapter.

15-2 LIGAND EQUILIBRIA

Macroscopic and microscopic constants

Before discussing the association of ligands with multiple sites on macromolecules, it is useful to discuss briefly the distinction between microscopic and macroscopic equilibrium constants. A concrete example is provided by the titration of the amino acid glycine. This can be viewed as a dibasic acid. We define GH_2^+, GH, and G^- as the forms bearing two, one, and no protons, respectively. The *macroscopic* equilibria are

$$GH_2^+ \rightleftarrows GH + H^+ \tag{15-1a}$$

$$GH \rightleftarrows G^- + H^+ \tag{15-1b}$$

and the two macroscopic dissociation constants are given by

$$K_1 = (GH)(H^+)/(GH_2^+) \tag{15-2a}$$

$$K_2 = (G^-)(H^+)/(GH) \tag{15-2b}$$

The two pK values can be obtained from a titration; at 25°C, extrapolated to zero ionic strength, they are $pK_1 = 2.35$, and $pK_2 = 9.78$.

We now examine the *microscopic* states of glycine during the titration. Altogether there are four forms, where

$$GH_2^+ = {}^+H_3NCH_2COOH \tag{15-3a}$$

$$GH = {}^+H_3NCH_2COO^- + H_2NCH_2COOH \tag{15-3b}$$

$$G^- = H_2NCH_2COO^- \tag{15-3c}$$

and the microscopic ionization equilibria are

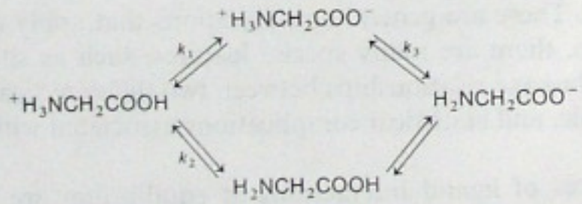

(15-4)

where the k_i values are microscopic dissociation constants. According to Equations 15-2 and 15-3,

$$K_1 = [({}^+H_3NCH_2COO^-) + (H_2NCH_2COOH)](H^+)/({}^+H_3NCH_2COOH) = k_1 + k_2 \tag{15-5a}$$

$$K_2 = (H_2NCH_2COO^-)(H^+)/[({}^+H_3NCH_2COO^-) + (H_2NCH_2COOH)] = 1/(k_3^{-1} + k_4^{-1}) \tag{15-5b}$$

Equation 15-5 shows the relationships between the microscopic and macroscopic dissociation constants.

The four microscopic constants are not independent. In particular,

$$k_1 k_3 = k_2 k_4 \tag{15-6}$$

Equation 15-6 is easy to verify; it is a direct consequence of detailed balancing. Equations 15-5 and 15-6 give three relationships involving the four microscopic constants. A fourth relationship may be obtained by assuming that k_2 has the same value as the single dissociation constant for the methyl ester of glycine (${}^+H_3NCH_2CO_2CH_3 \rightleftarrows H_2NCH_2CO_2CH_3 + H^+$). This assumption gives $pk_2 = 7.7$. With the values of pK_1 and pK_2 given earlier, it then is easy to calculate from Equations 15-5 and 15-6 that $pk_1 = 2.35$, $pk_3 = 9.78$, and $pk_4 = 4.43$. From these values, the reader should be able to deduce whether dissociation from ${}^+H_3NCH_2COOH$ to neutral glycine proceeds predominantly by the top path or the bottom path in Equation 15-4.

This simple illustration serves as a concrete example of the meanings of microscopic and macroscopic constants, and of their interrelationships. As a second example, we treat a situation in which *statistical effects* come into play. Consider a molecule A, which has two equivalent sites for a specific ligand. For instance, A might be a long-chain aliphatic dicarboxylic acid in which the microscopic dissociation constant is the same for each carboxylic group, regardless of the ionization state of the other group (this condition can be fulfilled if the aliphatic chain is long enough that electrostatic interactions between the two carboxyl groups are negligible). The macroscopic equilibria are

$$A + H^+ \rightleftarrows A(H^+)_1 \tag{15-7a}$$

$$A(H^+)_1 + H^+ \rightleftarrows A(H^+)_2 \tag{15-7b}$$

and the macroscopic dissociation constants are given by

$$K_1 = (A)(H^+)/(A(H^+)_1) \tag{15-8a}$$

$$K_2 = (A(H^+)_1)(H^+)/(A(H^+)_2) \tag{15-8b}$$

The microscopic equilibria can be written schematically as

$$A + H^+ \rightleftarrows AH^+ \tag{15-9a}$$

$$A + H^+ \rightleftarrows {}^+HA \tag{15-9b}$$

$$AH^+ + H^+ \rightleftarrows {}^+HAH^+ \tag{15-9c}$$

$${}^+HA + H^+ \rightleftarrows {}^+HAH^+ \tag{15-9d}$$

where the microscopic dissociation constant k is the same for each step. In Equation 15-9 we have distinguished between microspecies by assigning one ionization site to the left and the other to the right side of A. In terms of microscopic species, the macroscopic forms are defined as

$$A = A \tag{15-10a}$$

$$A(H^+)_1 = AH^+ + {}^+HA \tag{15-10b}$$

$$A(H^+)_2 = {}^+HAH^+ \tag{15-10c}$$

From Equations 15-8 to 15-10, we conclude that

$$K_1 = k/2 \tag{15-11a}$$

$$K_2 = 2k \tag{15-11b}$$

$$K_1/K_2 = 1/4 \tag{15-11c}$$

Thus, even though the microscopic dissociation constant is the same for each ionization, statistical effects make the first apparent macroscopic dissociation constant *four times smaller* than that of the second one.

In this chapter and in Chapter 17, we frequently use the concepts of microscopic and macroscopic constants, and it will be important to keep firmly in mind the distinctions between them that are illustrated in the preceding examples.

15-3 IDENTICAL INDEPENDENT SITES

Calculating the number of microscopic species

We first consider a macromolecule M, which contains n sites for the ligand L. Each site has the same microscopic ligand dissociation constant k. The sites also are assumed to be independent—that is, the microscopic dissociation constant k for a particular site is the same regardless of the state of occupancy of the other sites. The equilibria that characterize the interaction may be written as

$$\begin{aligned} M_0 + L &\rightleftarrows M_1 \\ M_1 + L &\rightleftarrows M_2 \\ &\vdots \\ M_{n-1} + L &\rightleftarrows M_n \end{aligned} \tag{15-12}$$

where the index on M denotes the total number of molecules of L that are bound. Thus, M_i is taken to mean the *total set of microscopic species that have i bound molecules of L*. For example, if $n = 4$, and we schematically represent our macromolecule as a square with four sites,

$$M_2 = \square\!\!\begin{matrix}\square & \text{L}\\ \text{L} & \square\end{matrix} + \square\!\!\begin{matrix}\square & \text{L}\\ \text{L} & \square\end{matrix} + \square\!\!\begin{matrix}\text{L} & \text{L}\\ \square & \square\end{matrix} + \square\!\!\begin{matrix}\square & \square\\ \text{L} & \text{L}\end{matrix} + \square\!\!\begin{matrix}\text{L} & \square\\ \square & \text{L}\end{matrix} + \square\!\!\begin{matrix}\text{L} & \square\\ \text{L} & \square\end{matrix} \tag{15-13}$$

where each microscopic form is present in equal amounts. Thus, with $n = 4$, there are six microscopic species that comprise M_2. In general, there are $\Omega_{n,i}$ distinct ways to put i ligands on n sites, where[§]

$$\Omega_{n,i} = \frac{n \times (n-1) \times (n-2) \times \cdots \times (n-i+1)}{i!} = \frac{n!}{(n-i)!i!} \tag{15-14}$$

Consequently, there are $\Omega_{n,i}$ microscopic forms that make up M_i.

Calculation of v

Equilibrium measurements of ligand binding typically yield the moles of ligand bound per mole of macromolecule. This parameter generally is designated v; it is given by

$$v = \sum_{i=0}^{n} i(M_i) \Big/ \sum_{i=0}^{n} (M_i) \tag{15-15}$$

Our goal is to express v in terms of the free ligand concentration, (L).

In general, we can express the concentration of any form M_i in terms of any

[§] Equation 15-14 is easy to derive. There are n different sites in which to place the first ligand; after it has been placed, there are $n - 1$ sites available for the second, then $n - 2$ for the third, and so on, with $n - i + 1$ sites available for the ith ligand. The product $n \times (n-1) \times \cdots \times (n-i+1)$ would give the total arrangements possible except that there is a redundancy; this arises because we have counted each distinct arrangement of i ligands in n sites more than once. For example, if we place the first ligand in site 4 and the second in site 2, this gives the same end result as if we had placed the first in site 2 and the second in site 4. In the product $n \times (n-1) \times \cdots \times (n-i+1)$, we have counted each distinct arrangement $i!$ times, so a correction must be made.

Note also that $\Omega_{n,i}$ is the binomial coefficient of x^i in the expansion of $(1 + x)^n$.

other form by making use of the *macroscopic* dissociation constants. For example,

$$K_1 = (M_0)(L)/(M_1) \tag{15-16a}$$

$$\vdots \qquad \vdots$$

$$K_i = (M_{i-1})(L)/(M_i) \tag{15-16b}$$

$$\vdots \qquad \vdots$$

$$K_n = (M_{n-1})(L)/(M_n) \tag{15-16c}$$

and

$$(M_i) = (M_{i-1})(L)/K_i = (M_0)(L)^i \Big/ \prod_{j=1}^{i} K_j \tag{15-17}$$

The macroscopic constant K_i is to be distinguished from the single microscopic constant k that characterizes all of the sites. The dissociation constant k refers to the equilibrium with respect to particular microscopic species, whereas the macroscopic constant K_i involves the entire ensemble of species represented by M_i and M_{i-1}. For example, with $n = 4$, and again using the format of the schematic illustration from Equation 15-13,

$$k = \frac{\left(\square\right)(L)}{\left(\square\right)} = \frac{\left(\square\right)(L)}{\left(\square\right)} = \frac{\left(\square\right)(L)}{\left(\square\right)} = \cdots \tag{15-18}$$

whereas K_1, for example, is

$$K_1 = \frac{\left(\square\right)(L)}{\left(\square\right) + \left(\square\right) + \left(\square\right) + \left(\square\right)} \tag{15-19}$$

The relationship between K_i and k is governed by the simple statistical factors $\Omega_{n,i}$. In particular, it is easy to show (Problem 15-1) that

$$K_i = (\Omega_{n,i-1}/\Omega_{n,i})k \tag{15-20}$$

Therefore, we can rewrite Equation 15-17 as

$$(M_i) = (M_{i-1})(L)/K_i = (M_{i-1})[(n - i + 1)/i][(L)/k] \tag{15-21}$$

With similar expressions for (M_{i-1}), (M_{i-2}), etc., we obtain

$$(M_i) = (M_0)\left\{\prod_{j=1}^{i} [(n - j + 1)/j]\right\}[(L)/k]^i \tag{15-22}$$

Substitution of Equation 15-22 into Equation 15-15 gives

$$v = \frac{\sum_{i=1}^{n} i\left\{\prod_{j=1}^{i} [(n - j + 1)/j]\right\}[(L)/k]^i}{1 + \sum_{i=1}^{n} \left\{\prod_{j=1}^{i} [(n - j + 1)/j]\right\}[(L)/k]^i} \tag{15-23}$$

Although Equation 15-23 appears algebraically complex, it readily simplifies. The product term is identical to $\Omega_{n,i}$ (Eqn. 15-14):

$$\prod_{j=1}^{i} [(n - j + 1)/j] = n!/(n - i)!i! \tag{15-24}$$

Substituting Equation 15-24 into Equation 15-23, we obtain

$$v = \frac{\sum_{i=1}^{n} i[n!/(n - i)!i!][(L)/k]^i}{1 + \sum_{i=1}^{n} [n!/(n - i)!i!][(L)/k]^i} \tag{15-25}$$

The denominator of Equation 15-25 is simply the binomial expansion of $[1 + (L)/k]^n$:

$$[1 + (L)/k]^n = 1 + \sum_{i=1}^{n} [n!/(n - i)!i!][(L)/k]^i \tag{15-26}$$

Differentiation of Equation 15–26 with respect to $(L)/k$, followed by multiplication by $(L)/k$, gives

$$n[(L)/k][1 + (L)/k]^{n-1} = \sum_{i=1}^{n} i[n!/(n - i)!i!][(L)/k]^i \tag{15-27}$$

The right-hand side of Equation 15-27 corresponds to the numerator of Equation 15-25. Substituting Equations 15-26 and 15-27 into Equation 15-25, we obtain

$$\boxed{v = \frac{n(L)/k}{1 + (L)/k}} \tag{15-28}$$

or

$$\boxed{v/(L) = n/k - v/k} \tag{15-29}$$

The simple forms of Equations 15-28 and 15-29 suggest that these expressions can be derived without recourse to the statistical framework we have generated. This is indeed the case, although the derivation just given is useful in that it gives good insight into the statistical features of the binding equilibria.

A simple derivation

An easy way to derive Equation 15-28 is to focus on the binding equilibrium of site i only. Let Θ_i be the fractional saturation of site i. Then,

$$\Theta_i = (\text{Bound site } i)/[(\text{Free site } i) + (\text{Bound site } i)]$$

$$= \frac{(\text{Free site } i)[(\text{Bound site } i)/(\text{Free site } i)]}{(\text{Free site } i)[1 + (\text{Bound site } i)/(\text{Free site } i)]} \tag{15-30}$$

Because (Bound site i)/(Free site i) = (L)/k, we have

$$\Theta_i = \frac{(\text{L})/k}{1 + (\text{L})/k} \tag{15-31}$$

A similar expression may be written for each of the n identical sites. Adding these n expressions together, we obtain Equation 15-28 (note that $\sum_i \Theta_i = v$).

Scatchard plot

Equation 15-29 is a useful representation of the relationship between v and (L) for the simple case of identical independent sites. A plot of v/(L) versus v is sometimes known as a Scatchard plot (see Scatchard, 1949). This plot is linear with an ordinate intercept of n/k, an abscissa intercept of n, and a slope of $-k^{-1}$ (Fig. 15-1). Clearly, this plot provides a simple and convenient way to obtain the two parameters that characterize the binding equilibria.

15-4 MULTIPLE CLASSES OF INDEPENDENT SITES

Curved Scatchard plots

In many cases, a Scatchard plot of v/(L) versus v proves to be curved rather than linear. This may mean that more than one class of sites are present. If there are n_1 independent sites with the intrinsic microscopic dissociation constant k_1, and n_2

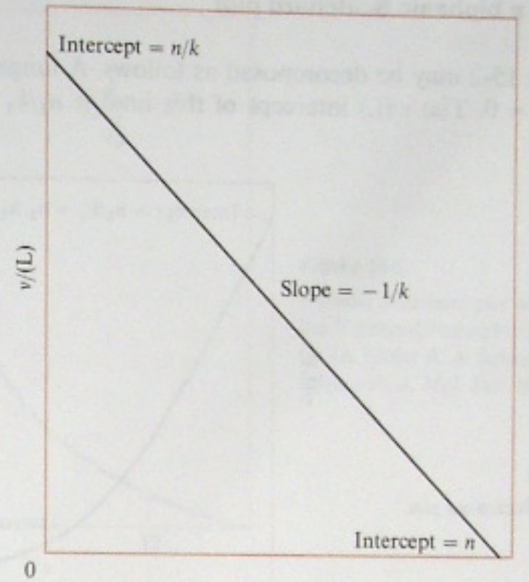

Figure 15-1
Scatchard plot for identical, independent binding sites.

sites with dissociation constant k_2, and so on, then an equation analogous to Equation 15-28 holds for each class of sites. Thus we obtain

$$v = \sum_i \frac{n_i(\text{L})/k_i}{1 + (\text{L})/k_i} \tag{15-32}$$

and

$$v/(\text{L}) = \sum_i \frac{n_i/k_i}{1 + (\text{L})/k_i} \tag{15-33}$$

Equations 15-32 and 15-33 are parametric forms that may be used to obtain the parameters n_i and k_i from a Scatchard plot. Figure 15-2 is an illustration of a biphasic plot for the case of two classes of independent sites.

Decomposition of a biphasic Scatchard plot

The plot in Figure 15-2 may be decomposed as follows. A tangent line is drawn to the plot around $v = 0$. The $v/(L)$ intercept of this line[§] is $n_1/k_1 + n_2/k_2$. As a first approximation, we can assume that it is dominated by the smallest k (defined as k_1) and estimate that the intercept is equal to n_1/k_1. Likewise, the v intercept of the tangent line is taken to be a first estimate of n_1. With estimates of n_1 and k_1, we can subtract from the data the contribution of the strongest-binding (smallest-k) sites. We then can construct a new plot that can be analyzed according to Equation 15-29 in order to obtain estimates of n_2 and k_2.

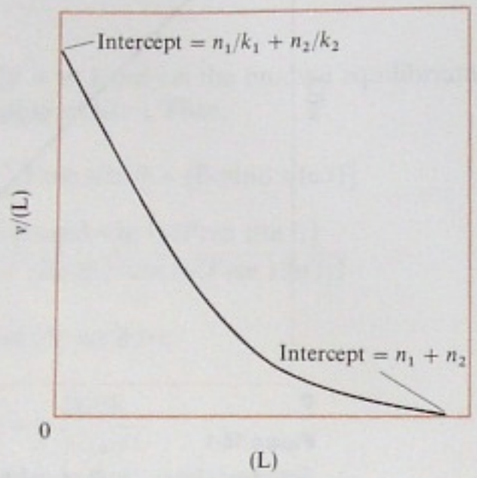

Figure 15-2
A biphasic Scatchard plot.

The first estimate of all the parameters may be improved by a refinement process. For example, a new estimate of n_1/k_1 may be obtained by subtracting the approximate values of n_2/k_2 from the $v/(L)$ intercept of the tangent line mentioned above. After this, the process can be continued to obtain a new estimate of n_2 and k_2. Throughout the procedure, the constraint is used that $n_1 + n_2$ equals the observed v intercept. The refinement procedure is continued until $\sum_i (n_i/k_i)$ equals the observed $v/(L)$ intercept.

Figure 15-3 gives data for the binding of Mn^{2+} to the 5′-(three-fifths molecule) of a specific transfer RNA in 0.1 M triethanolamine. Based on the tRNA cloverleaf

[§] The ratio $v/(L)$ appears to go to 0/0 when $(L) \to 0$. The value of this indeterminate form can be obtained from l'Hôpital's rule, which says that the limiting ratio is given by the limit of the derivative of the numerator (v) divided by the derivative of the denominator, (L). From Equation 15-32, $[dv/d(L)]_{(L)\to 0} = \sum_i n_i/k_i$, and $d(L)/d(L) = 1$; therefore,

$$\lim_{(L)\to 0} [v/(L)] = \sum_i n_i/k_i$$

This result also is obtained by letting $(L) \to 0$ on the right-hand side of Equation 15-33.

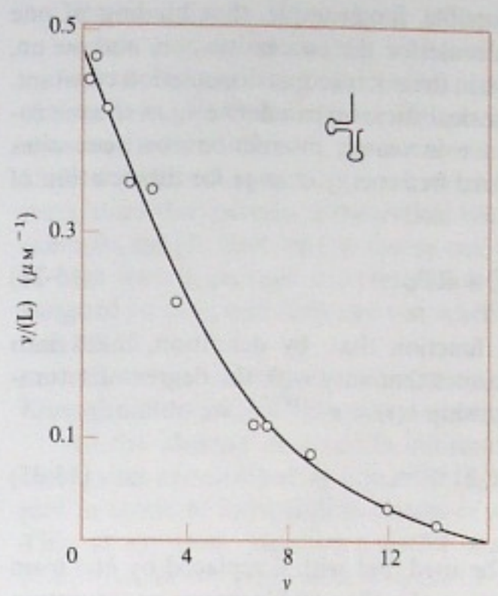

Figure 15-3
Biphasic Scatchard plot of Mn^{2+} binding to the 5′-(three-fifths molecule) of a specific tRNA. [After A. A. Schreier and P. R. Schimmel, *J. Mol. Biol.* 86:601 (1974).]

structure, this nucleic acid fragment contains single-stranded regions and a double-helical hairpin stem and hairpin loop. The data were analyzed as just described to give two classes of sites with $n_1 = 6$ and $n_2 = 10$; the dissociation constants are $k_1 = 14$ μM and $k_2 = 200$ μM. The curve is constructed from these calculated parameters, whereas the points are experimental. Good agreement is achieved between the calculated and observed behaviors.

Are the parameters obtained from a multiphasic Scatchard plot unique? For example, could other n_i and k_i values equally well fit the data in Figure 15-3? With the constraint that $n_1 + n_2 =$ constant, variations of ± 1 in n_i give relatively small (less than $\pm 50\%$) changes in the k_i values for this particular example. This suggests that the k_i values are reliable. A related question is whether the data might also be described well by positing more than two classes of sites. Of course, the greater the number of parameters available to fit any data to a model, the better will be the agreement between theory and experiment. The best procedure is to account for data, within the limits of experimental error, with the fewest possible assumptions and parameters. This approach gives a picture of the minimal (and presumably dominant) features of the system.

15-5 INTERACTION BETWEEN SITES

Some general considerations

Now we must ask whether the assumption of separate classes of sites, and the representation of Equations 15-32 and 15-33, is the only way to account for curved

Scatchard plots. It clearly is not. It is possible, for example, that binding of one ligand alters the affinity of the macromolecule for the successive one, and so on, effectively producing a continuous variation in the microscopic dissociation constant.

For the simple case of one class of identical sites, we can define k_0 as the microscopic dissociation constant at $v = 0$. As v increases, interactions between sites cause a change in k. Let ΔG^0 be the standard free energy change for dissociation of a bound ligand. This is given by

$$\Delta G^0 = \Delta G_0^0 + RT\phi(v) \tag{15-34}$$

where $\Delta G_0^0 = -RT \ln k_0$, and $\phi(v)$ is a function that, by definition, takes into account the effects of interactions between sites that vary with the degree of saturation. From Equation 15-34, and the relationship $k(v) = e^{-\Delta G^0/RT}$, we obtain

$$k(v) = k_0 e^{-\phi(v)} \tag{15-35}$$

where $\phi(v)$ is zero at $v = 0$.

Equations 15-28 and 15-29 can now be used, but with k replaced by $k(v)$ from Equation 15-35. If $\phi(v)$ is a decreasing function of v, then $k(v)$ increases as saturation proceeds. In this case, the Scatchard plot according to Equation 15-29 will be curved, concave upwards. On the other hand, if $\phi(v)$ increases as v increases, then the Scatchard plot can be "humped," or concave downwards. As binding proceeds, successive ligands are bound more strongly (smaller dissociation constants). This situation corresponds to one in which a cooperative interaction between sites occurs as v increases. Figure 15-4 illustrates the two cases.

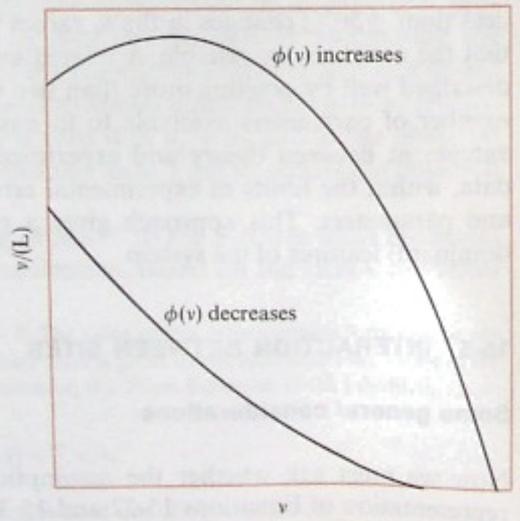

Figure 15-4
Hypothetical Scatchard plots for cases where $\phi(v)$ decreases or increases with increasing v.

Because $\phi(v)$ is a completely arbitrary function, it can always be defined so as to explain any data according to Equations 15-28 and 15-35. In an ideal situation, enough is known about the system under investigation that one can reasonably choose between the description of Equation 15-35 or the assumption of independent classes of sites as the best way to account for a curved Scatchard plot. If Equation 15-35 is believed to be the best description, then it is desirable to have a model for the system that permits a theoretical derivation of the functional form of $\phi(v)$. For example, simple electrostatic theory can be used to estimate $\phi(v)$ for the association of ions with a charged macromolecule (see Tanford, 1961). With a definite form assigned to $\phi(v)$, one then can test whether the data actually do conform to Equation 15-35.

However, in many situations it is not possible to derive an expression for $\phi(v)$. Enough information about the system simply is not available.

In the absence of accurate information on (or evidence for) negatively interacting sites as described by Equation 15-35, it is best to treat a concave-up Scatchard plot in terms of independent classes of sites (according to Eqns. 15-32 and 15-33). This, at the least, provides a useful phenomenological description of the system. Moreover, in any given situation, the likelihood of genuinely distinct classes of sites may be self-evident. In the example of Figure 15-3, the macromolecule under investigation presumably contains both single-stranded and double-stranded sections. Because the two types of sections are known to have significantly different ligand (Mn^{2+}) affinities, a model with at least two classes of sites is physically reasonable. If, as in the example, the data can be quantitatively accounted for by the different classes of sites known to exist in the macromolecule, then there is no reason to invoke possible effects due to $\phi(v)$.

However, in the event of a concave-down Scatchard plot (Fig. 15-4), separate classes of noninteracting sites cannot be assumed. This is because the description of Equations 15-32 and 15-33 gives only concave-up plots. Therefore, a concave-down plot is definitive evidence for interactions between sites: $\phi(v)$ decreasing with increasing v. We treat such systems in following subsections.

In the general case where there are several classes of interacting sites, then Equations 15-32 and 15-33 apply, with each k_i replaced by $k_i(v)$ where, by analogy with Equation 15-35,

$$k_i(v) = k_{0i} e^{-\phi_i(v)} \tag{15-36}$$

where k_{0i} is the intrinsic microscopic dissociation constant at $v = 0$ for sites in class i, and $\phi_i(v)$ is the interaction function for sites in class i. The interaction function for each class of sites may be unique, so that $\phi_i(v)$ can be different from $\phi_j(v)$. Of course, Equations 15-32 and 15-33, in conjunction with Equation 15-36, are useful only if enough information is available that $\phi_i(v)$ is known for each of the various classes of sites.

The preceding discussion serves to sketch the general issues that must be considered in treating interacting sites. In practice, cooperative interactions are probably

the most commonly encountered examples of interacting sites. These are considered next.

Prevalence of cooperative interactions

There are many examples in biology of the association of ligands with a macromolecule being a cooperative process. One of the best-studied examples is the association of oxygen with hemoglobin, discussed in greater depth in Chapter 17. In addition, many multisubunit enzymes bind substrates or other molecules in a cooperative fashion. The enzyme aspartate transcarbamoylase (also considered in Chapter 17) exhibits this kind of behavior. And, in some instances, certain nucleic acids cooperatively bind particular ligands. Thus, *cooperative interactions are widespread in biological systems.*

The cooperative association of ligands with macromolecules has been treated by many authors. Some aspects of these treatments, and some of the models for cooperativity put forth, are discussed in Chapter 17. At this point, however, it is worth considering some of the elementary features of these kind of interactions.

Statistical effects and interaction energy

For the sake of illustration, consider a macromolecule that combines with four ligands, L. If all of the sites are identical and independent and bind L with a microscopic dissociation constant k, then, according to Equation 15-20, the four macroscopic constants are

$$K_1 = (1/4)k \tag{15-37a}$$

$$K_2 = (2/3)k \tag{15-37b}$$

$$K_3 = (3/2)k \tag{15-37c}$$

$$K_4 = 4\,k \tag{15-37d}$$

Therefore, in this case, $K_1 < K_2 < K_3 < K_4$; that is, viewed from the standpoint of the macroscopic constants, the binding appears to become progressively weaker as saturation proceeds, even though the same microscopic constant holds for each site. Thus, from the standpoint of the macroscopic dissociation constants, statistical effects introduce some apparent *anticooperativity* into the binding equilibria.

In a cooperative system, when corrected for statistical effects, the apparent dissociation constant for one or more of the successive steps decreases as saturation progresses. In the example of a macromolecule with four sites, this means that, if cooperativity occurs between the first and second step, then (as a consequence of Eqn. 15-37) $4K_1 > (3/2)K_2$; if all four steps involve progressively stronger binding, then $4K_1 > (3/2)K_2 > (2/3)K_3 > (1/4)K_4$.

The magnitude of the cooperativity involved in binding two ligands can be cast into units of energy by a simple procedure. Let $\Delta G_i^0 = RT \ln K_i$ be the apparent standard free energy change for binding the ith ligand in a series. (Recall that K_i is a *dissociation* constant, so that $-RT \ln K_i$ is the free energy change associated with *dissociation*; therefore, $+RT \ln K_i$ is that associated with *association*.) This free energy change contains a pure statistical component given by $RT \ln (\Omega_{n,i-1}/\Omega_{n,i})$ (cf. Eqn. 15-20). To correct for this, we define the intrinsic standard free energy change associated with binding of the ith ligand in a series as $\Delta \bar{G}_i^0$, which is

$$\Delta \bar{G}_i^0 = +RT \ln K_i - RT \ln(\Omega_{n,i-1}/\Omega_{n,i}) \tag{15-38}$$

We define the interaction energy $\Delta G_{I,ij}$ per site as the difference in the intrinsic free energies of association of the ith and jth ligands. This interaction energy is

$$\begin{aligned} \Delta G_{I,ij} &= \Delta \bar{G}_j^0 - \Delta \bar{G}_i^0 \\ &= -RT \ln(K_i/K_j) + RT \ln\left(\frac{\Omega_{n,i-1}/\Omega_{n,i}}{\Omega_{n,j-1}/\Omega_{n,j}}\right) \end{aligned} \tag{15-39}$$

With this definition of $\Delta G_{I,ij}$, if the jth ligand binds more strongly than the ith ($j > i$), then as in a cooperative system, $\Delta G_{I,ij} < 0$. Note also that, if each site has the same intrinsic dissociation constant, then the two terms on the right-hand side of Equation 15-39 cancel, and $\Delta G_{I,ij} = 0$.

In the case of oxygen binding to human hemoglobin, Equation 15-39 gives $\Delta G_{I,ij} \cong -2$ kcal mole^{-1} site^{-1} for $i = 1$ and $j = 4$. This means that site–site interactions stabilize a bound oxygen molecule in the saturated hemoglobin tetramer by approximately 2 kcal mole^{-1} over an oxygen molecule bound to a hemoglobin species that has three vacant sites.

A semiempirical approach: the Hill constant

For the purpose of treating and characterizing data on the cooperative association of ligands, it is common practice to use a semiempirical approach and then to interpret the physical significance of the empirical parameters that are obtained. This approach is based on the assumption that the binding over part of the saturation range can be described by equations phenomenologically resembling those for an infinitely cooperative system. In the extreme case of infinite cooperativity, the binding can be represented as an "all-or-none" reaction:

$$M_0 + nL \rightleftarrows M_n \tag{15-40}$$

$$K^n = (M_0)(L)^n/(M_n) \tag{15-41}$$

where K is the apparent dissociation constant for the interacting sites. For this case, the parameter v is given by

$$v = n(\mathrm{M}_n)/[(\mathrm{M}_0) + (\mathrm{M}_n)]$$
$$= [n(\mathrm{L})^n/K^n]/[1 + (\mathrm{L})^n/K^n] \quad (15\text{-}42a)$$

$$v/(\mathrm{L}) = [n(\mathrm{L})^{n-1}/K^n]/[1 + (\mathrm{L})^n/K^n] \quad (15\text{-}42b)$$

whereas the fractional saturation $\bar{y} = v/n$ is

$$\bar{y} = [(\mathrm{L})^n/K^n]/[1 + (\mathrm{L})^n/K^n] \quad (15\text{-}43)$$

Equations 15-40 through 15-43 are based on the assumption that binding is infinitely cooperative for all n ligands. In practice, infinite cooperatively is not observed. Instead, data on cooperative interactions commonly are described over part of the saturation range (typically 25% to 75%) by semiempirical relationships analogous to Equations 15-40 through 15-43. These semiempirical relationships are

$$v = [n(\mathrm{L})^{\alpha_H}/K^{\alpha_H}]/[1 + (\mathrm{L})^{\alpha_H}/K^{\alpha_H}] \quad (15\text{-}44a)$$

$$v/(\mathrm{L}) = [n(\mathrm{L})^{\alpha_H - 1}/K^{\alpha_H}]/[1 + (\mathrm{L})^{\alpha_H}/K^{\alpha_H}] \quad (15\text{-}44b)$$

$$\bar{y} = [(\mathrm{L})^{\alpha_H}/K^{\alpha_H}]/[1 + (\mathrm{L})^{\alpha_H}/K^{\alpha_H}] \quad (15\text{-}45)$$

where $1 \leqslant \alpha_H \leqslant n$. *The parameter α_H commonly is known as the Hill constant* (see Hill, 1910); it is an index to the cooperativity. When $\alpha_H = n$, the system behaves as perfectly cooperative, whereas $\alpha_H = 1$ indicates no cooperativity. Figure 15-5 shows several plots of $\bar{y}$ versus $(\mathrm{L})/K$ for various values of α_H. It is clear that the steepness of the curve is very sensitive to α_H.

From Equation 15-45, the parameter α_H is given by

$$\frac{d\{\ln[\bar{y}/(1-\bar{y})]\}}{d[\ln(\mathrm{L})]} = \alpha_H \quad (15\text{-}46)$$

Equation 15-46 serves as a convenient definition of the Hill constant. In general, Equation 15-45 does not hold over the entire range of values of $\bar{y}$, so that α_H is a

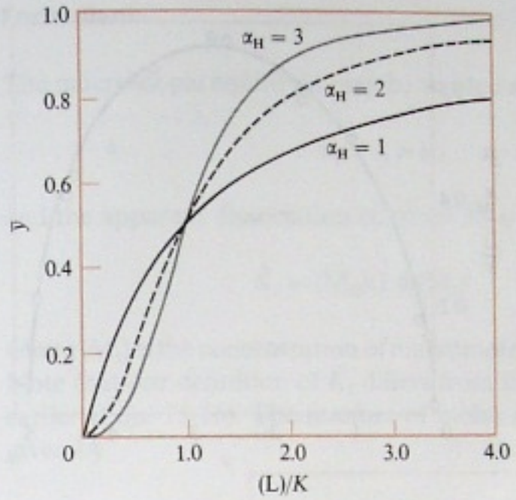

Figure 15-5
Effect of α_H on fractional saturation curves.

function of the degree of saturation. Often the parameter α_H is evaluated at $\bar{y} = 1 - \bar{y} = 1/2$. In this case, Equation 15-46 becomes (note that $d\ln x = dx/x$)

$$\left(\frac{d[\bar{y}/(1-\bar{y})]}{d(\mathrm{L})}\right)_{\bar{y}=1/2} = \frac{\alpha_{H,1/2}}{(\mathrm{L})_{1/2}} \quad (15\text{-}47)$$

where $(\mathrm{L})_{1/2}$ is the concentration of L at half-saturation, and $\alpha_{H,1/2}$ is the value of α_H when $\bar{y} = 1/2$. Equations 15-46 and 15-47 are useful relationships; they show that the Hill constant can be obtained from the slope of a plot of $\ln[\bar{y}/(1-\bar{y})]$ versus $\ln(\mathrm{L})$, which is called a Hill plot.

Equation 15-44 gives parametric relationships that can be used to analyze Scatchard plots of cooperative associations, sometimes over a broad range of values of v and (L). These plots are markedly different from those discussed earlier for independent, noninteracting sites. According to Equation 15-44b, for $\alpha_H > 1$ the plot actually passes through the origin—as when $v = 0$ [or $(\mathrm{L}) = 0$] and $v/(\mathrm{L}) = 0$. At low values of v or (L), the curve rises and reaches a maximum at $v_{max} = n(\alpha_H - 1)/\alpha_H$, and then descends to intercept the v axis at $v = n$.

Figure 15-6 shows an example of this kind of Scatchard plot. This figure gives data on the cooperative association of Mn^{2+} to transfer RNA. The concave-down character of the plot is clearly evident. Parameters that characterize the interaction may be obtained by defining K^{α_H} in terms of experimentally determined variables as follows:

$$K^{\alpha_H} = (\mathrm{L})^{\alpha_H}[n(\mathrm{M})_0 - (\mathrm{L})_b]/(\mathrm{L})_b \quad (15\text{-}48)$$

and rearranging Equation 15-48 to give

$$\ln(\mathrm{L}) = -(1/\alpha_H)\ln[(n/v) - 1] + \ln K \quad (15\text{-}49)$$

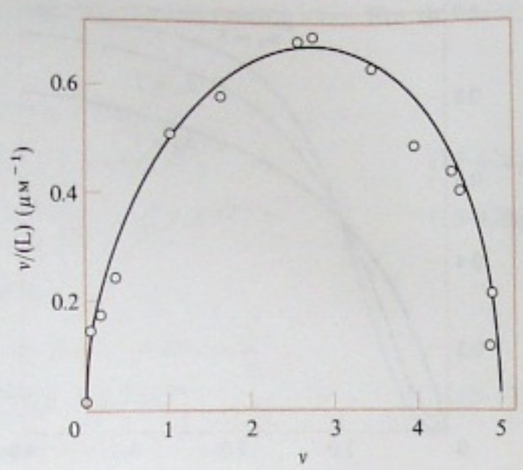

Figure 15-6
Scatchard plot of Mn^{2+} binding to a specific tRNA. [After A. A. Schreier and P. R. Schimmel, *J. Mol. Biol.* 86:601 (1974).]

where $(L)_b$ is the concentration of bound ligand, $(M)_0$ is the total macromolecule concentration, and $\nu = (L)_b/(M)_0$. It is clear from Equation 15-49 that a plot of ln(L) versus $\ln[(n/\nu) - 1]$ should give a straight line with slope of $-1/\alpha_H$ and intercept of $-\ln K$. The linearity is very sensitive to the value of n assumed, so that a good check is obtained on the value of n determined from the Scatchard plot. When the data in Figure 15-6 are plotted according to Equation 15-49, the parameters $n = 5$, $\alpha_H = 2.3$, and $K = 3.7$ μM are found to describe the data accurately. These data show that Mn^{2+} binding is cooperative, and that about five sites are involved; however, they do not act in a wholly "all-or-none" fashion, because $\alpha_H < n$. This is analogous to oxygen binding to hemoglobin, where α_H is 2.5 to 3.0 and $n = 4$.

Although not considered further here, these data and other results are particularly useful in constructing a model for the association of cations with tRNA (see Schimmel, 1976).

15-6 BINDING OF TWO DIFFERENT LIGANDS: LINKED FUNCTIONS

Thus far we have considered only situations in which one kind of ligand binds to a macromolecule. However, there are situations encountered in practice where the simultaneous binding of two different ligands must be considered. One example is the effect of pH on ligand binding. In this instance, the binding of H^+ to one or more critical sites is closely linked to the association of ligand.

When two different ligands bind to a macromolecule, there is an interesting and useful set of interrelationships that describe the binding equilibria. Our treatment follows lines developed by J. Wyman (1964). We start by considering again the binding of a single ligand L to n sites on a macromolecule M. We use a somewhat different formalism than that developed earlier; this one is particularly useful for treating linked equilibria.

Formalism

The macroscopic equilibria may be written as follows:

$$M_0 + iL \rightleftarrows M_i \qquad \text{for } i = 1, 2, \ldots, n \tag{15-50}$$

and the apparent dissociation constant $\tilde{K}_i$ is

$$\tilde{K}_i = (M_0)(L)^i/(M_i) \qquad \text{for } i = 1, 2, \ldots, n \tag{15-51}$$

where (M_i) is the concentration of macromolecules that have i bound ligand molecules. Note that our definition of $\tilde{K}_i$ differs from that of the macroscopic constant K_i used earlier (Eqn. 15-16). The number of moles of L bound per mole of M is $n\bar{y}$ and is given by

$$n\bar{y} = \frac{\sum_{i=0}^{n} i(M_i)}{\sum_{i=0}^{n} (M_i)} = \frac{\sum_{i=0}^{n} [i(L)^i/\tilde{K}_i]}{\sum_{i=0}^{n} [(L)^i/\tilde{K}_i]} \tag{15-52}$$

$$n\bar{y} = \frac{d\left(\ln \sum_{i=0}^{n} [(L)^i/\tilde{K}_i]\right)}{d[\ln(L)]} \tag{15-53}$$

where $\tilde{K}_0$ is equal to unity. Equation 15-53 is a particularly useful form.

Each $\tilde{K}_i$ is related to the microscopic constants that characterize the binding to each of the n sites on M. Letting the microscopic constants be distinct and designated as $k_1, k_2, \ldots, k_n$, we can easily show (Problem 15-5) that

$$\sum_{i=0}^{n} [(L)^i/\tilde{K}_i] = [1 + (L)/k_1][1 + (L)/k_2] \cdots [1 + (L)/k_n] \tag{15-54}$$

If every $k_i = k$, then

$$\sum_{i=0}^{n} [(L)^i/\tilde{K}_i] = [1 + (L)/k]^n \tag{15-55}$$

and, from Equation 15-53,

$$\bar{y} = [(L)/k]/[1 + (L)/k] \tag{15-56}$$

Equation 15-56 is identical to Equation 15-28, with $\bar{y} = \nu/n$.

Two ligands and a basic linkage relationship

Assume now that there are two ligands, L_1 and L_2. There are n sites for L_1 and m sites for L_2. Let $\bar{y}_1$ be the fractional saturation with respect to L_1, and $\bar{y}_2$ be that with respect to L_2. We define the macroscopic equilibrium constant $\tilde{K}_{ij}$ for the equilibrium

$$iL_1 + jL_2 + M_0 \rightleftarrows M_{ij} \tag{15-57}$$

as

$$\tilde{K}_{ij} = (L_1)^i(L_2)^j(M_0)/(M_{ij}) \tag{15-58}$$

where M_{ij} has i molecules of L_1 and j molecules of L_2 bound to it, and M_0 has neither ligand bound. Note that $K_{00} = 1$. The parameter $n\bar{y}_1$ thus is given by

$$n\bar{y}_1 = \frac{\sum_{i=0}^{n}\sum_{j=0}^{m} i(M_{ij})}{\sum_{i=0}^{n}\sum_{j=0}^{m}(M_{ij})} \tag{15-59}$$

Using Equation 15-58, we obtain

$$n\bar{y}_1 = \frac{\sum_{i=0}^{n}\sum_{j=0}^{m}[i(L_1)^i(L_2)^j/\tilde{K}_{ij}]}{\sum_{i=0}^{n}\sum_{j=0}^{m}[(L_1)^i(L_2)^j/\tilde{K}_{ij}]} \tag{15-60}$$

or

$$n\bar{y}_1 = \left(\frac{\partial\left\{\ln\sum_i\sum_j[(L_1)^i(L_2)^j/\tilde{K}_{ij}]\right\}}{\partial[\ln(L_1)]}\right)_{(L_2)} \tag{15-61}$$

Likewise, for $m\bar{y}_2$ we have

$$m\bar{y}_2 = \left(\frac{\partial\left\{\ln\sum_i\sum_j[(L_1)^i(L_2)^j/\tilde{K}_{ij}]\right\}}{\partial[\ln(L_2)]}\right)_{(L_1)} \tag{15-62}$$

For given $\tilde{K}_{ij}$ values, the double sum in Equation 15-61 or 15-62 is a function only of (L_1) and (L_2). Therefore, we have

$$d(\ln\textstyle\sum\sum) = \left(\frac{\partial\sum\sum}{\partial[\ln(L_1)]}\right)_{(L_2)} d[\ln(L_1)] + \left(\frac{\partial\sum\sum}{\partial[\ln(L_2)]}\right)_{(L_1)} d[\ln(L_2)] \tag{15-63}$$

$$d(\ln\textstyle\sum\sum) = n\bar{y}_1\, d[\ln(L_1)] + m\bar{y}_2\, d[\ln(L_2)] \tag{15-64}$$

where $\sum\sum$ denotes the double sum in the numerator of Equation 15-61 or 15-62. By cross-differentiation (Box 15-1) of Equation 15-64, we obtain

$$\boxed{n\left(\frac{\partial\bar{y}_1}{\partial[\ln(L_2)]}\right)_{(L_1)} = m\left(\frac{\partial\bar{y}_2}{\partial[\ln(L_1)]}\right)_{(L_2)}} \tag{15-65}$$

Equation 15-65 is a basic linkage relationship. It shows that, at constant (L_1), a rise in (L_2) changes the number of moles of bound L_1 by an amount exactly equal to the change in the number of moles of bound L_2 accompanying an increase in (L_1) at constant (L_2).

Another equation for the linkage effect

Of the four variables $\bar{y}_1$, $\bar{y}_2$, (L_1), and (L_2), only two are independent. Therefore, it is possible to transform Equation 15-65 into alternative forms. A particularly useful one involves the derivative $(\partial\bar{y}_1/\partial\bar{y}_2)_{(L_1)}$, which by the chain rule (Box 15-2) is

$$(\partial\bar{y}_1/\partial\bar{y}_2)_{(L_1)} = (\partial\bar{y}_1/\partial[\ln(L_2)])_{(L_1)}(\partial[\ln(L_2)]/\partial\bar{y}_2)_{(L_1)} \tag{15-66}$$

Box 15-1 CROSS-DIFFERENTIATION

For a function $f(x, y)$ of two independent variables x and y,

$$\begin{aligned} df &= (\partial f/\partial x)_y\, dx + (\partial f/\partial y)_x\, dy \\ &= f_x\, dx + f_y\, dy \end{aligned}$$

where $f_x = (\partial f/\partial x)_y$, and $f_y = (\partial f/\partial y)_x$. The cross-differentiation relationship says that

$$(\partial f_x/\partial y)_x = (\partial f_y/\partial x)_y$$

This follows from the second-derivative relationships:

$$(\partial f_x/\partial y)_x = \frac{\partial}{\partial y}(\partial f/\partial x)_y = \frac{\partial^2}{\partial y\partial x}f = \frac{\partial^2}{\partial x\partial y}f = \frac{\partial}{\partial x}(\partial f/\partial y)_x = (\partial f_y/\partial x)_y$$

Substituting Equation 15-65 into Equation 15-66, we obtain

$$(\partial\bar{y}_1/\partial\bar{y}_2)_{(L_1)} = (m/n)(\partial\bar{y}_2/\partial[\ln(L_1)])_{(L_2)}(\partial[\ln(L_2)]/\partial\bar{y}_2)_{(L_1)} \quad (15\text{-}67)$$

The derivative with respect to $\bar{y}_2$ on the right-hand side of Equation 15-67 can be evaluated from the total differential for $d\bar{y}_2$:

$$d\bar{y}_2 = (\partial\bar{y}_2/\partial[\ln(L_1)])_{(L_2)}\, d[\ln(L_1)] + (\partial\bar{y}_2/\partial[\ln(L_2)])_{(L_1)}\, d[\ln(L_2)] \quad (15\text{-}68)$$

At constant $\bar{y}_2$, we have $d\bar{y}_2 = 0$, and Equation 15-68 gives

$$(\partial[\ln(L_2)]/\partial\bar{y}_2)_{(L_1)} = -(\partial[\ln(L_1)]/\partial\bar{y}_2)_{(L_2)}(\partial[\ln(L_2)]/\partial[\ln(L_1)])_{\bar{y}_2} \quad (15\text{-}69)$$

Substituting Equation 15-69 into Equation 15-67, we obtain

$$\left(\frac{\partial[\ln(L_2)]}{\partial[\ln(L_1)]}\right)_{\bar{y}_2} = -\frac{n}{m}\left(\frac{\partial\bar{y}_1}{\partial\bar{y}_2}\right)_{(L_1)} \quad (15\text{-}70)$$

The quantity $n\,d\bar{y}_1$ is the change in the number of occupied L_1 sites, and $-n\,d\bar{y}_1 = d[n(1-\bar{y}_1)]$ is the change in the number of free L_1 sites. Therefore, Equation 15-70 says that the expression on the left-hand side of the equation is the change in the number of free L_1 sites (or the number of moles of L_1 released) upon binding of a mole of L_2. Of course, the number released can be positive or negative (negative release corresponds to binding).

The derivative on the left-hand side of Equation 15-70 is experimentally accessible. Figure 15-7 shows plots of $\bar{y}_2$ versus $\ln(L_2)$ for different values of $\ln(L_1)$.

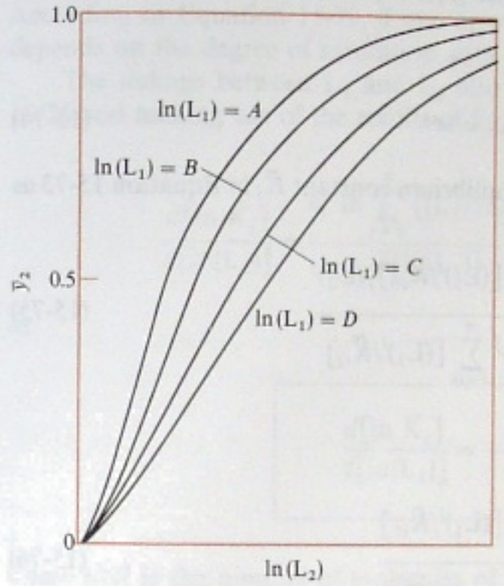

Figure 15-7
Hypothetical plots of $\bar{y}_2$ versus $\ln(L_2)$ for different values of $\ln(L_1)$.

The ligand L_1 could be H^+, for example, and the curves then would simply illustrate the familiar observation that ligand binding (L_2 in this case) is affected by pH. Clearly, the horizontal difference between two adjacent curves divided by $\Delta[\ln(L_1)]$ gives the desired derivative. An analogous plot for the linked binding of oxygen and diphosphoglycerate to hemoglobin is given in Chapter 17 (Fig. 17-21). In that case, L_2 = oxygen and L_1 = diphosphoglycerate.

An additional relationship

In order to grasp concretely how the coupling between ligands takes place, it is helpful to extend our analysis in a somewhat different way. Let us denote by $M^{(j)}$ all species that have j bound L_2 molecules. Therefore,

$$(M^{(j)}) = \sum_{i=0}^{n} (M_{ij}) \quad (15\text{-}71)$$

Box 15-2 THE CHAIN RULE

Consider a system of four variables (f, g, x, and y) of which only two can be independent. Choose x and y as independent variables. We then have

$$df = (\partial f/\partial x)_y\, dx + (\partial f/\partial y)_x\, dy \quad (A)$$

$$dg = (\partial g/\partial x)_y\, dx + (\partial g/\partial y)_x\, dy \quad (B)$$

Because x and y are independent, they can be varied at will. Choose y to be fixed, so that $dy = 0$; then divide Equation A by Equation B to obtain

$$(\partial f/\partial g)_y = (\partial f/\partial x)_y/(\partial g/\partial x)_y \quad (C)$$

$$(\partial f/\partial g)_y = (\partial f/\partial x)_y(\partial x/\partial g)_y \quad (D)$$

Equation D is the chain-rule relationship, so named because the two derivatives on the right-hand side of Equation D appear to form a chain.

and, using Equation 15-58,

$$(M^{(j)}) = (M_0)(L_2)^j \sum_{i=0}^{n} [(L_1)^i/\tilde{K}_{ij}] \tag{15-72}$$

We define the equilibrium constant $\bar{K}_j$ as

$$\bar{K}_j = (M^{(0)})(L_2)^j/(M^{(j)}) \tag{15-73}$$

which corresponds to the reaction

$$M^{(0)} + jL_2 \rightleftarrows M^{(j)} \tag{15-74}$$

Using Equation 15-72, we can write the equilibrium constant $\bar{K}_j$ in Equation 15-73 as

$$\bar{K}_j = \frac{\{(M_0) \sum_{i=0}^{n} [(L_1)^i/\tilde{K}_{i0}]\}(L_2)^j}{(M_0)(L_2)^j \sum_{i=0}^{n} [(L_1)^i/\tilde{K}_{ij}]} \tag{15-75}$$

After cancellations, we obtain

$$\bar{K}_j = \frac{\sum_{i=0}^{n} [(L_1)^i/\tilde{K}_{i0}]}{\sum_{i=0}^{n} [(L_1)^i/\tilde{K}_{ij}]} \tag{15-76}$$

If each microscopic constant for the binding of L_2 to M is distinct, then (by analogy with Eqn. 15-54)

$$\sum_{i=0}^{n} [(L_1)^i/\tilde{K}_{ij}] = (1/\tilde{K}_{0j})([1 + (L_1)/k_{11}][1 + (L_1)/k_{12}] \cdots [1 + (L_1)/k_{1n}])_{M^{(j)}} \tag{15-77}$$

and

$$\sum_{i=0}^{n} [(L_1)^i/\tilde{K}_{i0}] = ([1 + (L_1)/k_{11}][1 + (L_1)/k_{12}] \cdots [1 + (L_1)/k_{1n}])_{M^{(0)}} \tag{15-78}$$

where k_{1p} denotes the microscopic dissociation constant for L_1 at site p, and the subscript $M^{(j)}$ outside the brackets denotes that the microscopic constants pertain to the species with j bound L_2 molecules. Thus, the microscopic constants for L_1 binding in general can vary according to how many L_2 molecules are bound. Using Equations 15-77 and 15-78, we obtain for Equation 15-76

$$\bar{K}_j = \tilde{K}_{0j} \frac{\prod_{i=1}^{n} (1 + (L_1)/k_{1i})_{M^{(0)}}}{\prod_{i=1}^{n} (1 + (L_1)/k_{1i})_{M^{(j)}}} \tag{15-79}$$

According to Equation 15-79, if one or more of the microscopic constants for L_1 depends on the degree of saturation with L_2, then $\bar{K}_j$ depends on (L_1).

The linkage between L_1 and L_2 also can be seen by differentiating Equation 15-76 and making use of the results of Equations 15-52 and 15-53 to obtain

$$\frac{d[\ln \bar{K}_j]}{d[\ln(L_1)]} = \frac{d \left\{ \ln \sum_{i=0}^{n} [(L_1)^i/\tilde{K}_{i0}] \right\}}{d[\ln(L_1)]} - \frac{d \left\{ \ln \sum_{i=0}^{n} [(L_1)^i/\tilde{K}_{ij}] \right\}}{d[\ln(L_1)]} \tag{15-80}$$

or

$$\boxed{\frac{d[\ln \bar{K}_j]}{d[\ln(L_1)]} = -n(\bar{y}_1^{(j)} - \bar{y}_1^{(0)})} \tag{15-81}$$

where $n\bar{y}_1^{(j)}$ is the number of molecules of L_1 bound to molecules of M that have j bound L_2 molecules. Thus the expression on the right-hand side of Equation 15-81 gives the number of L_1 molecules released upon binding of j L_2 molecules to M. However, according to Equation 15-79, if

$$\prod_{i=1}^{n} (1 + (L_1)/k_{1i})_{M^{(0)}} = \prod_{i=1}^{n} (1 + (L_1)/k_{1i})_{M^{(j)}}$$

then $\bar{K}_j = \tilde{K}_{0j}$, and $d[\ln \bar{K}_j]/d[\ln(L_1)] = 0$. Hence, *linkage between* L_1 *and* L_2 *binding occurs if the microscopic constants for binding of one ligand are influenced by the amount of the other ligand that is bound.*

These types of interrelationships between ligand bindings are well illustrated in the case of hemoglobin and the Bohr effect. In this case, there is strong linkage between oxygen binding and the binding of "Bohr" protons (see Chapter 17). Another example is provided by the hydrolysis of ATP, where both reactant and products can complex with Mg^{2+} and H^+. R. A. Alberty (1969) summarizes this interesting system.

15-7 LINKAGE OF LIGAND BINDING FROM AN ENERGETIC VIEWPOINT

Coupling free energy

Gregorio Weber (1975) has used a different viewpoint for examining coupled ligand equilibria, treating them in terms of energetic considerations. This treatment helps us to think concretely in terms of the energies involved in the linked reactions.

For the sake of illustration, consider a simple system in which a macromolecule binds one molecule each of ligands L_1 and L_2. The reactions are

$$M + L_1 \rightleftarrows ML_1 \qquad \Delta G_1^0 \qquad (15\text{-}82a)$$

$$M + L_2 \rightleftarrows L_2M \qquad \Delta G_2^0 \qquad (15\text{-}82b)$$

$$L_2M + L_1 \rightleftarrows L_2ML_1 \qquad \Delta G_1^0(2) \qquad (15\text{-}82c)$$

$$ML_1 + L_2 \rightleftarrows L_2ML_1 \qquad \Delta G_2^0(1) \qquad (15\text{-}82d)$$

Standard free energies for each of the reactions are indicated on the right-hand side; for example, $\Delta G_1^0(2)$ is the standard free energy change for binding L_1 to the macromolecule saturated with L_2.

The free energies in Equation 15-82 are not independent, but are tied together because

$$\Delta G_1^0 + \Delta G_2^0(1) = \Delta G_2^0 + \Delta G_1^0(2) = \Delta G^0(1,2) \qquad (15\text{-}83)$$

where $\Delta G^0(1,2)$ is the standard free energy change for the reaction

$$M + L_1 + L_2 \rightleftarrows L_2ML_1 \qquad (15\text{-}84)$$

Figure 15-8 is a diagram of these relationships. Note that there is no requirement that $\Delta G_1^0 = \Delta G_1^0(2)$ or that $\Delta G_2^0 = \Delta G_2^0(1)$. From Equation 15-83, we have

$$\Delta G_1^0(2) - \Delta G_1^0 = \Delta G_2^0(1) - \Delta G_2^0 \equiv \Delta G_{12}^0 \qquad (15\text{-}85)$$

The meaning of this equation is similar to the linkage relationship of Equation 15-65 for the case $m = n = 1$. It says that the effect (in terms of free energy) of L_2 on the binding of L_1 is the same as the effect of L_1 on the binding of L_2. This mutual effect of one ligand on the other can be put in terms of a coupling free energy ΔG_{12}^0 (defined in Eqn. 15-85).

Combining Equations 15-83 and 15-85, we obtain another expression for ΔG_{12}^0:

$$\Delta G_{12}^0 = \Delta G^0(1,2) - \Delta G_1^0 - \Delta G_2^0 \qquad (15\text{-}86)$$

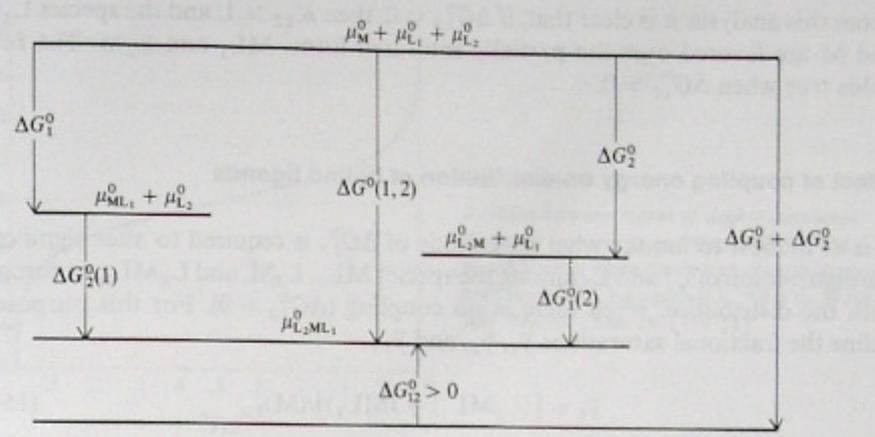

Figure 15-8

Free energy diagram for a system of two ligands, L_1 and L_2, and a macromolecule M. Each ligand has one site on the macromolecule. Standard chemical potentials are designated μ^0 with subscripts referring to particular species. [After G. Weber, *Adv. Protein Chem.* 29:1 (1975).]

Thus, ΔG_{12}^0 is the difference between (a) the standard free energy for the overall reaction $M + L_1 + L_2 \rightleftarrows L_2ML_1$, and (b) the sum of the standard free energies for the reactions $M + L_1 \rightleftarrows ML_1$ and $M + L_2 \rightleftarrows L_2M$. Figure 15-8 shows the definition of ΔG_{12}^0.

Clearly, if $\Delta G_{12}^0 = 0$, there is no interaction between ligands; binding of each proceeds in a truly independent fashion. For other cases, the sign of the coupling free energy determines whether the interaction between ligands is *cooperative* or *antagonistic*. If $\Delta G_{12}^0 < 0$, then binding of either L_1 or L_2 facilitates binding of the other ligand. Conversely, when $\Delta G_{12}^0 > 0$, there is antagonism between the bindings of the ligands.

There is still another way to look at the coupling free energy. To do this, we write out the three relevant equilibria and their associated free energy changes:

$$L_1 + L_2 + M \rightleftarrows L_2ML_1 \qquad \Delta G^0(1,2) \qquad (15\text{-}87a)$$

$$L_1 + M \rightleftarrows ML_1 \qquad \Delta G_1^0 \qquad (15\text{-}87b)$$

$$L_2 + M \rightleftarrows L_2M \qquad \Delta G_2^0 \qquad (15\text{-}87c)$$

Subtracting Equation 15-87b,c from 15-87a, we obtain

$$ML_1 + L_2M \rightleftarrows M + L_2ML_1 \qquad \Delta G^0(1,2) - \Delta G_1^0 - \Delta G_2^0 = \Delta G_{12}^0 \qquad (15\text{-}88)$$

Thus, ΔG_{12}^0 is the free energy change for a kind of disproportionation reaction. This reaction has an equilibrium constant K_{12} given by

$$K_{12} = e^{-\Delta G_{12}^0/RT} = (L_2ML_1)(M)/(ML_1)(L_2M) \qquad (15\text{-}89)$$

From this analysis, it is clear that, if $\Delta G^0_{12} < 0$, then $K_{12} > 1$, and the species L_2ML_1 and M are favored over the partially saturated forms ML_1 and L_2M. The reverse holds true when $\Delta G^0_{12} > 0$.

Effect of coupling energy on distribution of bound ligands

It is of interest to inquire what magnitude of ΔG^0_{12} is required to alter significantly the distribution of L_1 and L_2 among the species ML_1, L_2M, and L_2ML_1, as compared with the distribution when there is no coupling ($\Delta G^0_{12} = 0$). For this purpose, we define the fractional saturations $\bar{y}_1$, $\bar{y}_2$, and $\bar{y}_{12}$:

$$\bar{y}_1 = [(L_2ML_1) + (ML_1)]/(M)_{Tot} \tag{15-90a}$$

$$\bar{y}_2 = [(L_2ML_1) + (L_2M)]/(M)_{Tot} \tag{15-90b}$$

$$\bar{y}_{12} = (L_2ML_1)/(M)_{Tot} \tag{15-90c}$$

where $(M)_{Tot} = (M) + (ML_1) + (L_2M) + (L_2ML_1)$. Clearly, $\bar{y}_1$ and $\bar{y}_2$ are the overall fractional saturations with respect to L_1 and L_2, and $\bar{y}_{12}$ is the degree of double saturation.

Consider a situation where (L_1) and (L_2) are so adjusted that one-half of the L_1 sites and one-half of the L_2 sites are filled. Under these conditions, it is easy to show (see Problem 15-4) that

$$K_{12} = \bar{y}^2_{12}/[(1/2) - \bar{y}_{12}]^2 \tag{15-91}$$

and

$$\bar{y}_{12} = (1/2)K^{1/2}_{12}/(1 + K^{1/2}_{12}) \tag{15-92}$$

Substituting Equation 15-91 into Equation 15-89, we obtain

$$\Delta G^0_{12} = -2RT \ln[2\bar{y}_{12}/(1 - 2\bar{y}_{12})] \tag{15-93}$$

From Equation 15-93 we can obtain a plot of ΔG^0_{12} versus $2\bar{y}_{12}$ (Fig. 15-9). When $2\bar{y}_{12} = 1$, all of the bound ligands are in the form of L_2ML_1. When $2\bar{y}_{12} = 0$, all of the bound ligands are in the form of ML_1 and L_2M. At the point $2\bar{y}_{12} = 0.5$, we see that $\Delta G^0_{12} = 0$ (no coupling); this is the result expected for a simple unbiased statistical distribution of the ligands among ML_1, L_2M, and L_2ML_1, and where each species is present in equal amounts. Note that the plot in Figure 15-9 is symmetric about the point $2\bar{y}_{12} = 0.5$.

When $\Delta G^0_{12} = -2$ kcal mole^{-1}, then $2\bar{y}_{12}$ is greater than 0.8; when $\Delta G^0_{12} = -3$ kcal mole^{-1}, then $2\bar{y}_{12}$ is over 0.9. In the latter case, over 90% of the bound L_1 and L_2 is in the form of the double-saturated species L_2ML_1. In this instance, ligand

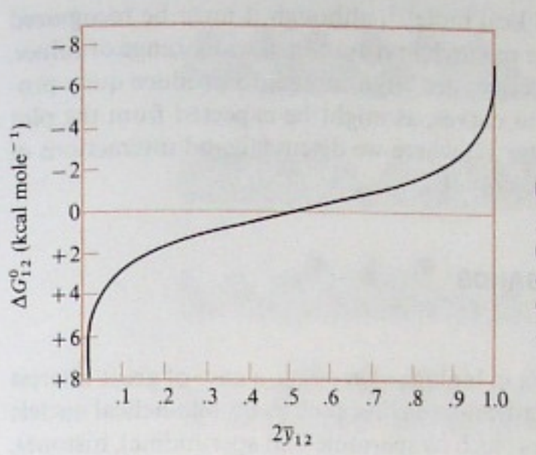

Figure 15-9
Relation between degree of double saturation ($\bar{y}_{12}$) and free energy coupling (ΔG^0_{12}) of the bound ligands, when the degree of saturation of each ligand ($\bar{y}_1$, $\bar{y}_2$) equals 0.5. [After G. Weber, *Adv. Protein Chem.* 29:1 (1975).]

binding proceeds largely from the species M to L_2ML_1, with little formation of ML_1 and L_2M. Conversely, when $\Delta G^0_{12} = +2$ or $+3$ kcal mole^{-1}, most of the species at half-saturation are the monoliganded forms ML_1 and L_2M. Thus, a coupling energy of only about ± 2 kcal mole^{-1} is sufficient to cause a substantial skewing of the distribution of liganded forms away from that obtained on a random basis.

Coupling free energies found in biological systems

Table 15-1 gives several examples of values for the coupling free energy between two different ligands that interact with a protein. Both positive and negative energies are found, corresponding to antagonistic and cooperative effects, respectively. The

Table 15-1
Free energy coupling between ligands

Protein	Ligand couple‡	ΔG^0_{12} (kcal mole^{-1})
Hemoglobin	Oxygen, 2,3-DPG	+1.3
Hemoglobin	Oxygen, IHP	+2.3
Serum albumin, bovine	ANS, 3,5-dihydroxybenzoate	+1.5
Pyruvate kinase	Phosphoenol pyruvate, K^+	−1.2
Pyruvate kinase	K^+, Mn^{2+}	−1.4
Pyruvate kinase	Phenylalanine, Mn^{II}	+0.8
Aspartate transcarbamoylase	CTP, succinate	+0.5
Lactate dehydrogenase, chicken heart	NADH, oxalate	−1.5

‡ IHP = inositol hexaphosphate; CTP = cytidine triphosphate; 2,3-DPG = 2,3-diphosphoglycerate; ANS = 1-anilinonaphthalene 8-sulfonate.
SOURCE: After G. Weber, *Adv. Protein Chem.* 29:1 (1975).

energies fall in the range of 0 to ± 2.5 kcal mole^{-1}, although it must be recognized that the data are sparse and that further research may turn up a wider range of values. At least in some cases, the coupling energies are large enough to produce quite pronounced effects in the ligand saturation curves, as might be expected from the plot in Figure 15-9 (and as shown in Chapter 17, where we discuss ligand interactions of aspartate transcarbamoylase and hemoglobin).

15-8 INTERACTION OF LARGE LIGANDS WITH LATTICELIKE CHAINS

In considering ligand binding equilibria in biological systems, a case of great interest is the association of large ligands with latticelike chains, such as double-helical nucleic acids. Large ligands include polyamines (such as spermine and spermidine), histones, DNA-unwinding proteins, and large drugs such as actinomycin D. These systems have special statistical features that are quite distinct from the situations described thus far. Moreover, they are amenable to a rather straightforward treatment, which we present along lines developed by J. D. McGhee and P. H. von Hippel (1974).

The homogeneous lattice: statistical features

Consider first a homogeneous lattice constructed of N identical repeating units. For example, in a helical nucleic acid, the repeating units could be phosphate groups or sugar units. Assume that one ligand L occupies l consecutive lattice units; saturation of the lattice with L results in N/l bound ligand molecules per lattice. The ligand is assumed to be able to occupy any l consecutive lattice units. Therefore, in the completely naked lattice, there are $N - l + 1$ potential sites that the first bound ligand can occupy. Thus, at the beginning of a ligand titration there are many more potential sites than the N/l sites that can be occupied at saturation. In this feature, this situation contrasts sharply with our earlier treatment of identical and independent sites (Eqn. 15-12), in which the number of free sites (n) on M_0 corresponds to the number that are filled on M_n. It is this aspect of the lattice that gives rise to a Scatchard plot markedly different from those obtained with the simple system of Equation 15-12.

Figure 15-10 illustrates the statistical complexities of the lattice for the case of $N = 12$ and $l = 3$. Let v represent the moles of L bound per mole of lattice. At saturation $v = N/l = 4$ bound ligand molecules per lattice. At the outset of titration, however, there are $N - l + 1 = 10$ potential sites per lattice. The figure shows that a variety of microspecies are generated after $v = 2$ bound ligands per lattice. Owing to the arrangement of ligands on the lattice, one species can accommodate no additional ligands, whereas others can take on two more. All of these species are in equilibrium with the free-ligand concentration, and they must be accounted for in any attempt to calculate the shape of the binding curve. Of course, as binding proceeds beyond $v = 2$, there must be a continual redistribution of the ligand on the lattice until the final state of $v = 4$ is reached.

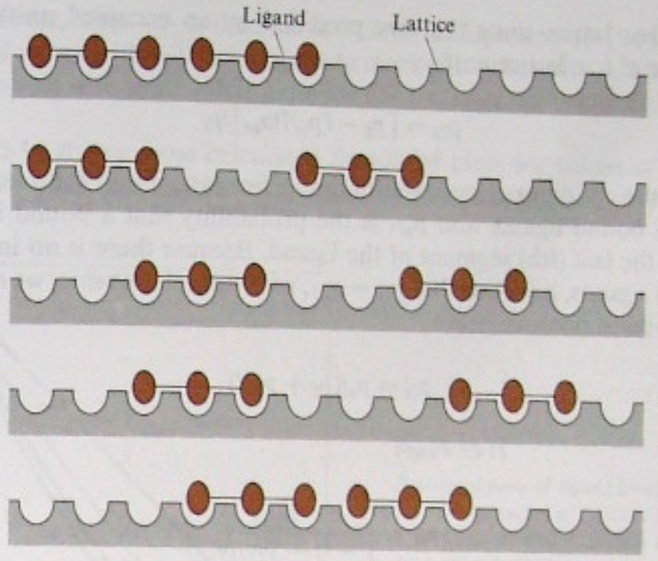

Figure 15-10

Some of the microspecies for the case of two ligands bound to the lattice, with $l = 3$ and $N = 12$.

Calculation of ligand-binding behavior

To calculate the ligand-binding behavior of the lattice, we start with the basic relationship

$$v = \bar{N}_{fl}(\mathrm{L})/k \tag{15-94}$$

where $\bar{N}_{fl}$ is the average number of free ligand sites of length l per lattice, and k is the intrinsic microscopic dissociation constant. Equation 15-94 follows directly from the definition of k. Our main task is to calculate an expression for $\bar{N}_{fl}$. We do this by first calculating the probability p_l that, starting at any position in the lattice, l *consecutive* lattice units are unoccupied with ligand; this probability times N gives the average number of free ligand sites of length l per lattice.

The probability p_l can be written as

$$p_l = p_f p_{ff}^{l-1} \tag{15-95}$$

where p_f is the probability that a lattice unit selected at random is unoccupied, and p_{ff} is the *conditional* probability that a given free unit is followed by another free unit. Because the fraction of occupied lattice units is vl/N, the fraction of unoccupied ones is $1 - vl/N$; therefore, p_b (the probability of occurrence of a bound unit) equals vl/N, and $p_f = 1 - vl/N$.

The conditional probability p_{ff} is also the fraction of the total free lattice units that are preceded by free units. This is [(total number of free lattice units) minus

(number of free lattice units that are preceded by an occupied unit)] divided by (total number of free lattice units):

$$p_{ff} = [p_f - (p_b/l)p_{bf}]/p_f \tag{15-96}$$

where p_{bf} is the conditional probability that a free lattice unit follows the last (lth) segment of a bound ligand, and p_b/l is the probability that a bound lattice unit is occupied by the last (lth) segment of the ligand. Because there is no interaction between bound ligands, it is clear that $p_{ff} = p_{bf}$; with this relationship, we can rearrange Equation 15-96 to obtain

$$p_{ff} = p_f/(p_f + p_b/l) \tag{15-97}$$

or

$$p_{ff} = \frac{1 - lv/N}{1 - (l-1)v/N} \tag{15-98}$$

We are now ready to obtain an expression for $\bar{N}_{fl}$:

$$\bar{N}_{fl} = Np_l = N(1 - lv/N)\left(\frac{1 - lv/N}{1 - (l-1)v/N}\right)^{l-1} \tag{15-99}$$

Equation 15-99 is obtained by using Equation 15-95 for p_l and the expressions for p_f and p_{ff}. Substituting Equation 15-99 into Equation 15-94, we obtain

$$\boxed{v/(\mathrm{L}) = \frac{N(1 - lv/N)}{k}\left(\frac{1 - lv/N}{1 - (l-1)v/N}\right)^{l-1}} \tag{15-100}$$

Equation 15-100 is the desired result. (Note that we ignored end effects in deriving this equation so that, strictly speaking, it is valid only for an infinite lattice. However, as we show in a subsequent section, Eqn. 15-100 affords a sufficiently accurate description for many systems of experimental interest involving finite lattices.)

Nonlinear Scatchard plots resulting from statistical effects

Equation 15-100 may be compared with the corresponding equation (Eqn. 15-29) for binding of L to n identical independent sites in which the "overlap" effect is not operative. When $l = 1$, Equation 15-100 reduces to Equation 15-29, as expected. (Note that, when $l = 1$, the n of Eqn. 15-29 equals the N of Eqn. 15-100; in general, $n = N/l$.) However, when $l > 1$, then the last factor in Equation 15-100 is always less than unity and varies with v. This gives rise to marked nonlinearity in Scatchard plots of $v/(\mathrm{L})$ versus v; it also means that plots for $l > 1$ always fall below the plot for the case $l = 1$.

Figure 15-11 shows some calculated Scatchard plots for values of l between 1 and 20, with $k = 1$ M. For ease in comparing the plots, the abscissa is given in units of $1/l$. In all cases, complete saturation is achieved when $v = n = N/l$. However, as l increases, the concave-up curvature of the plots becomes increasingly apparent. This happens because the lattice entropically resists being saturated, with the resistance becoming more pronounced as l increases. Thus, the statistically large number of microstates that are generated at a given degree of partial saturation gives a strong entropic contribution to the free energy. This is lost, of course, as binding proceeds to the completely saturated lattice, which is comprised of only one microstate. As a result, for large ligands, saturation is not practically feasible; for example, with $l = 10$ to 20, (L) must change by 10-fold to 100-fold in order to increase the lattice saturation merely from 80% to 90%.

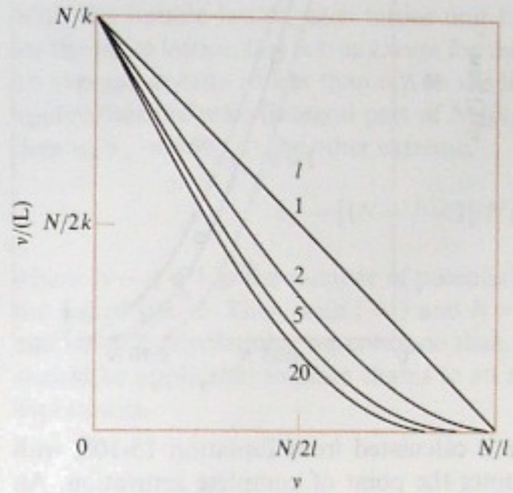

Figure 15-11
Scatchard plots of ligand binding to a lattice for various values of l with $k = 1$ M. [After J. D. McGhee and P. H. von Hippel, *J. Mol. Biol.* 86:469 (1974).]

The v intercept of the Scatchard plot is N/l, which corresponds to n in Equation 15-29. However, the $v/(\mathrm{L})$ intercept is N/k, which is not the same as n/k, the intercept given by Equation 15-29. This distinction is important to recognize when obtaining parameters from Scatchard plots involving ligand binding to latticelike chains.

Some results on a real system

Figure 15-12 shows some actual data. This figure gives the Scatchard plot for binding of an ε-dinitrophenyl (ε-DNP) oligomer of lysine, ε-DNP-Lys–$(\mathrm{Lys})_5$, to the

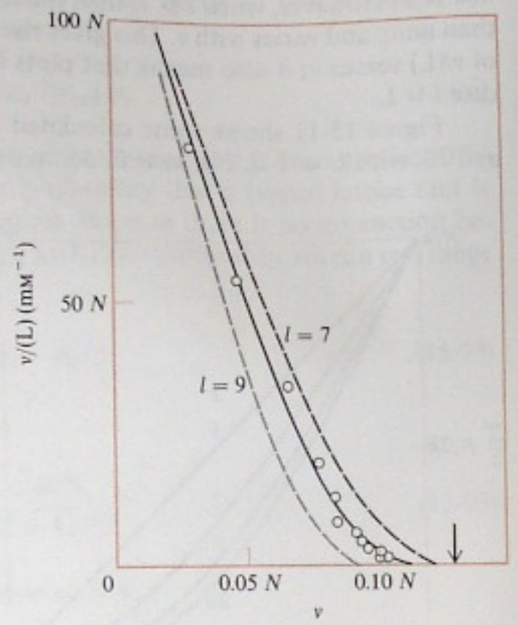

Figure 15-12

Scatchard plot for binding of ε-DNP-Lys-(Lys)$_5$ to the poly (rI):poly (rC) helix. Points are experimental values. The solid curve is calculated from Equation 15-100 with $l = 7.8$ and $k = 7.1$ μM. Dashed curves give calculated results with k held fixed and $l = 7$ or $l = 9$. The arrow denotes the point of lattice saturation. [After J. D. McGhee and P. H. von Hippel, *J. Mol. Biol.* 86:469 (1974).]

poly(rI):poly(rC) helix. The solid curve is calculated from Equation 15-100, with $l = 7.8$, and $k = 7.1$ μM. The arrow denotes the point of complete saturation. An excellent fit to the data is obtained. The dashed curves show the sensitivity of the data to variations in l with k held fixed. It is clear that a change of only about ± 1 from the best-fit value results in a marked departure of the calculated from the observed curve.

If a mixture of ligands bind to the lattice, then Equation 15-100 may be extended in a straightforward manner to handle this situation. Indexing by i the parameters associated with each ligand, we obtain

$$\nu_i/(\mathrm{L}_i) = \frac{N\left(1 - \sum_i l_i \nu_i \Big/ N\right)}{k_i} \left(\frac{1 - \sum_i l_i \nu_i \Big/ N}{1 - \sum_i (l_i - 1)\nu_i \Big/ N} \right)^{l_i - 1} \tag{15-101}$$

This equation can be used when separate means are available to measure the binding of each ligand. For example, if binding to a helix of two different polyamines (such as spermine and spermidine) is studied, the use of a ^{14}C label for one and a ^{3}H label for the other would be appropriate in a dialysis experiment. In other situations, ligands with distinct optical bands might be of use.

Lattices of finite length and end effects

Strictly speaking, Equations 15-100 and 15-101 are valid only in the limit that N goes to infinity. This is true because we ignored end effects in the derivation. We can

estimate the correction factor for any finite value of N. For this purpose, let $\nu/N = \nu_N$ be the saturation density of a lattice of N units, and ν_∞ be that for a lattice with an infinite number of units. Equation 15-100 then can be written as

$$\nu_\infty/(\mathrm{L}) = \frac{1 - l\nu_\infty}{k} \left(\frac{1 - l\nu_\infty}{1 - (l-1)\nu_\infty} \right)^{l-1} \tag{15-102}$$

With the infinite lattice, each lattice unit has an average saturation density of ν_∞: for the finite lattice, this is true *except* for the $l - 1$ units at each end, which can have an average density of less than ν_∞. In the limit of $(\mathrm{L}) \to \infty$, it is obvious that ν_N/ν_∞ approaches the ratio (integral part of N/l)$/(N/l)$. For example, if $l = 3$ and $N = 100$, then $\nu_N/\nu_\infty = 0.99$. At the other extreme,

$$\nu_N \to [(N - l + 1)/N]\nu_\infty \qquad \text{as } (\mathrm{L}) \to 0 \tag{15-103}$$

where $N - l + 1$ is the number of potential binding sites for a ligand of length l in the naked lattice. Thus, with $l = 3$ and $N = 100$, we have $\nu_N/\nu_\infty = 0.98$. From these and similar calculations, we conclude that, for values of $N/l \geqslant 30$, Equation 15-100 should be applicable to finite chains to an accuracy greater than that achievable by experiment.

Ligand–ligand interactions

In some cases, binding of a ligand to a lattice chain can be cooperative. This is true for some of the DNA-binding proteins. These situations too can be handled with the formalism we have developed. For this purpose, we must introduce a parameter that accounts for the ligand–ligand interaction on the lattice. Consider two partially saturated lattice microspecies with identical numbers of bound ligands. Moreover, we assume that the distributions of these ligands are exactly the same, except that a pair of isolated (not contiguous) ligands on lattice A are made contiguous on lattice B, so as to introduce only one new ligand–ligand interaction on lattice B. The lattice equilibrium is A ⇄ B, where

$$\omega = (\mathrm{B})/(\mathrm{A}) \tag{15-104}$$

Proceeding along lines similar to those used to derive Equation 15-100, we obtain

$$\frac{\nu}{(\mathrm{L})} = \frac{N(1 - l\nu/N)}{k} \left(\frac{(2\omega + 1)(1 - l\nu/N) + \nu/N - R}{2(\omega - 1)(1 - l\nu/N)} \right)^{l-1} \left(\frac{1 - (l+1)\nu/N + R}{2(1 - l\nu/N)} \right)^{2} \tag{15-105}$$

where

$$R = \{[1 - (l+1)\nu/N]^2 + (4\omega\nu/N)(1 - l\nu/N)\}^{1/2} \tag{15-106}$$

(For a more complete derivation, see McGhee and von Hippel, 1974.)

For the case of $\omega = 1$, Equation 15-105 can be shown to reduce to Equation 15-100. When $\omega < 1$ (anticooperative binding), Scatchard plots according to Equation 15-105 fall below those of the noninteracting case (Eqn. 15-100). When $\omega = 0$ (infinite anticooperativity), Equation 15-105 reduces to Equation 15-100 for noninteracting ligands with a length of $l + 1$ segments. When $\omega > 1$, the Scatchard plots are concave-down, and they fall above the corresponding noninteracting case. Figure 15-13 shows some plots for various values of ω with $l = 1$ and $k = 1$ M. Because these

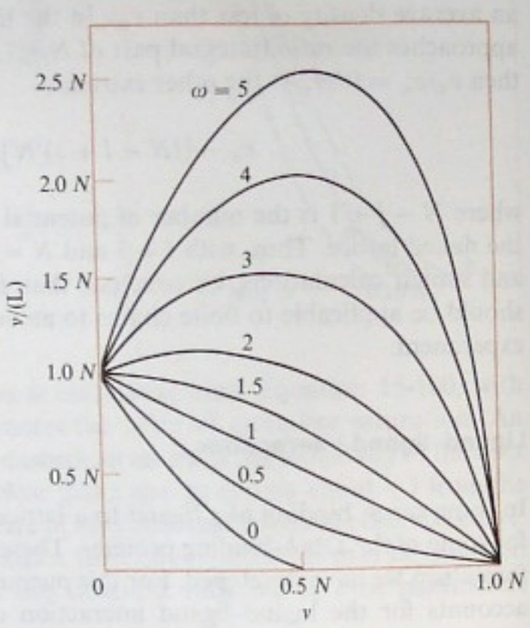

Figure 15-13

Scatchard plots for ligand binding to a homogenous lattice, for $k = 1$ M, and $l = 1$, with various values of the cooperativity parameter ω. [After J. D. McGhee and P. H. von Hippel, *J. Mol. Biol.* 86:469 (1974).]

curves are drawn for $l = 1$, these is no "overlap" effect mixed with the cooperativity. As shown earlier (Fig. 15-11), the effect of increasing l is to introduce an anticooperative feature into the binding. In a case where $\omega > 1$ and $l > 1$, the resulting curve obviously will be a compromise between the two parameters.

The ν/(L) intercept of the Scatchard plot of Equation 15-105 is N/k, the same as that for the noninteracting system described by Equation 15-100. Moreover, the ν intercept is still N/l. However, when $\omega > 1$, lattice saturation at any given value of n clearly is easier to achieve than in the noninteracting case ($\omega = 1$) where entropic effects inhibit saturation.

This treatment of ligand binding to a homogeneous lattice is applicable to a number of situations that are encountered in practice. Although another approach must be used to handle heterogeneous lattices, which have more than one type of ligand combining site, the above treatment does indicate that nonlinear regions in Scatchard plots can be explained in significant measure by the "overlap" effect. When

effects beyond those predicted by Equation 15-100 or 15-105 are observed, lattice heterogeneity must be considered. This requires a further extension of the theory.

In Chapter 23, where ligand binding to nucleic acids is considered further, we develop a different kind of treatment of ligand binding to lattices, based on matrix methods.

Summary

Ligand interactions are widespread in biochemical systems, and a rich and useful formalism has developed for treating the equilibrium properties of the diversity of systems that are encountered. In such treatments it is important to keep firmly in mind the distinction between microscopic and macroscopic constants, and associated statistical features. The simplest systems involve binding of a ligand to a single class of identical, independent sites. These can be analyzed conveniently by a Scatchard plot. An extension of the Scatchard type of analysis can be useful for treating multiple classes of independent sites.

In many biological systems, interactions occur between binding sites for a single kind of ligand. For example, cooperative interactions commonly are found, and they may be treated by established procedures. Another type of interaction is that between binding sites for different kinds of ligands that bind with the same macromolecule. In this case, particularly interesting and useful linkage relationships describe the interaction. The interaction energy that characterizes the linkage commonly is on the order of 0 to ± 2.5 kcal mole^{-1}.

Another case of considerable interest is the interaction of large ligands with latticelike chains, such as helical DNA. In such systems, statistical, entropic effects play a major role in determining the character of the observed binding equilibria.

Problems

15-1. The relationship shown by Equation 15-20 is useful in many calculations. Prove this relationship.

15-2. A ligand binds to four sites on a macromolecule. The apparent macroscopic dissociation constants K_2 and K_3 are identical (within experimental error). Is there an interaction energy between sites 2 and 3? If not, why not? If so, calculate the interaction energy.

15-3. A macromolecule has six sites for the ligand L. An investigator is able to measure three of the macroscopic dissociation constants for ligand binding, K_1, K_4, and K_5. He finds that $K_5 = 15K_1$, and $K_4 = 8K_1$. He then claims that this result clearly demonstrates negative (anticooperative) site–site interactions, and that the Scatchard plot for this

system is surely concave-up. A critic disagrees and says that the limited data indicate there are no site–site interactions, and he even ventures to predict relative K_i values for the other constants. Who is right, and why? Is it possible to predict the other K_i values? If so, make the predictions. If not, explain why none can be made.

15-4. Consider a case in which two ligands, L_1 and L_2, bind to a macromolecule. Let half of the L_1 and half of the L_2 sites be filled. Using Equations 15-89 and 15-90, derive Equations 15-91, 15-92, and 15-93.

15-5. The relationship shown by Equation 15-54 is a simple connection between microscopic dissociation constants, k_i, and macroscopic dissociation constants, $\tilde{K}_i$, defined in Equation 15-51. Establish the validity of Equation 15-54 for the case of three microscopic constants, k_1, k_2, and k_3, and of three macroscopic constants, $\tilde{K}_1$, $\tilde{K}_2$, and $\tilde{K}_3$, and reflect on the reason for the particularly simple form of Equation 15-54.

References

GENERAL

Alberty, R. A., and F. Daniels. 1979. *Physical Chemistry*, 5th ed. New York: Wiley. [Chaps. 4 and 6 give a good introduction to chemical equilibrium and biochemical equilibria.]

McGhee, J. D., and P. H. von Hippel. 1974. Theoretical aspects of DNA–protein interactions: cooperative and non-cooperative binding of large ligands to a one-dimensional homogeneous lattice. *J. Mol. Biol.* 86:469. [Includes an extremely clear exposition of ligand interactions with latticelike chains. The statistical complexities of the lattice are well discussed, and they are put in physically understandable terms.]

Wyman, J., Jr. 1964. Linked functions and reciprocal effects in hemoglobin: A second look. *Adv. Protein Chem.* 19:223. [A classical paper on ligand equilibria and linked functions.]

SPECIFIC

Alberty, R. A. 1969. Thermodynamics of the hydrolysis of adenosine triphosphate. *J. Chem. Ed.* 46:713.

Hess, V. L., and A. Szabo. 1979. Ligand binding to macromolecules: Allosteric and sequential models of cooperativity. *J. Chem. Ed.* 56:289. [A nice introduction to the use of generating functions to treat macromolecule–ligand systems.]

Hill, A. V. 1910. The possible effects of the aggregation of the molecules of hemoglobin on its dissociation curves. *J. Physiol. (London)* 40:iv.

Scatchard, G. 1949. The attraction of proteins for small molecules and ions. *Ann. N.Y. Acad. Sci.* 51:660.

Schimmel, P. R. 1976. Equilibrium and kinetic studies of the cooperative interaction of cations with transfer RNA. *J. Polymer Sci. Symp. No. 54*, p. 387.

Strandberg, M. W. P. 1979. Linear differential equations in chemical equilibrium calculations. *J. Chem. Phys.* 71:4765. [A differential equations approach is used to show certain general features of macromolecule–ligand systems.]

Tanford, C. 1961. *Physical Chemistry of Macromolecules*. New York: Wiley. [Chap. 8 treats multiple equilibria and complex systems, with many illustrations.]

Weber, G. 1975. Energetics of ligand binding to proteins. *Adv. Protein Chem.* 29:1.

16
Kinetics of ligand interactions

16-1 BIOCHEMICAL KINETIC STUDIES

The study of ligand interactions from an equilibrium standpoint (Chapter 15) gives insight into thermodynamic features and general mechanistic aspects of the ligand reactions. However, equilibrium measurements alone are not sufficient for a detailed mechanistic understanding of ligand reactions. In general, there are many possible reaction schemes that can account for a given set of thermodynamic data. These different schemes often can be sorted out by studies of the dynamics (or kinetics) of ligand reactions. Such investigations not only permit identification of reaction pathways that are followed, but they also can give quantitative insight into the time scale of elementary processes; from this information, it is possible to deduce a clearer picture of events at the molecular level.

All biochemical systems exhibit dynamic behavior. In many cases, the *physiological property* itself is in essence a *dynamic property*, as in enzyme catalysis, active ion transport across membranes, repression and activation of gene expression, and so on. For this reason, studies of the dynamic behavior of biochemical systems have been of great interest for many years.

In this chapter, we discuss some of the essential features of kinetic systems. Many of the ideas and equations developed here have applications in other chapters of the book. For example, in Chapter 21, where mechanisms for the folding of proteins are discussed, kinetic aspects are of great importance. In the following discussion, much of the treatment centers around enzymatic reaction systems, which have been investigated in more depth from a kinetic viewpoint than has any other class of biochemical systems. Also, as a concrete example of how an integration of kinetic